

# TNSA ion acceleration at $10^{16}$ W/cm<sup>2</sup> sub-nanosecond laser intensity

L Torrisi<sup>1,5</sup>, M Cutroneo<sup>1</sup>, L Calcagno<sup>2</sup>, M Rosinski<sup>3</sup> and J Ullschmied<sup>4</sup>

<sup>1</sup>Dep. of Physics-SdT, University of Messina, V. S. d'Alcontres 31, 98166 S. Agata (ME), Italy

<sup>2</sup>Dep. of Physics & Astronomy, University of Catania, V. S. Sofia 64, 95124 Catania, Italy

<sup>3</sup>Institute of Plasma Physics and Laser Microfusion, 23 Hery Street 01-497 Warsaw, Poland

<sup>4</sup>IPP ASCR - PALS, Za Slovankou 3, 182 00 Prague 8, Czech Republic

E-mail: Lorenzo.Torrisi@unime.it

**Abstract.** Micrometric thin targets have been irradiated in vacuum in TNSA (Target Normal Sheath Acceleration) configuration at PALS Laboratory in Prague by using  $10^{16}$  W/cm<sup>2</sup> laser intensity, 1315 nm wavelength, 300 ps pulse duration and different laser beam energies and focal positions. The plasmas produced were characterized by using ion collectors, semiconductor SiC detectors, X-ray streak camera and Thomson parabola spectrometer. Time of flight techniques, time resolved imaging and ion deflection spectrometry were used to characterize the laser-generated non-equilibrium plasma and the electric field driving ion acceleration developed at the rear side of the target. The maximum ion acceleration can be obtained for optimal film thickness depending on the laser energy and on the kind of irradiated targets. Special targets containing nanostructures, showing high absorption and low reflective coefficients, induce resonant absorption effects enhancing the electric acceleration field. The maximum kinetic energy measured for proton ions was above 5.0 MeV and the ion distributions can be fitted with Coulomb-Boltzmann shifted functions.

## 1. Introduction

The properties of the non-equilibrium plasma generated by pulsed laser-matter interaction in vacuum, using high laser intensities and TNSA (Target Normal Sheath Acceleration) configuration, depend strongly on three key parameters: the laser properties, irradiation conditions and target structure. The main laser properties are the intensity, wavelength, pulse duration and polarization direction [1]. The irradiation conditions are characterized by the laser spot dimensions, focal position of the laser with respect to the target surface, pressure in the vacuum irradiation chamber, use of prepulse or presence of gas leak, etc. [2]. Not less important is the role of the target structure because its material, thickness, geometry, and microscopic structure influence significantly the plasma composition, its temperature and density, and the number of fast electrons. All that plays a substantial role at optimising the ion

<sup>5</sup> To whom correspondence should be addressed



acceleration, through reduction of reflection effects, increase of absorption, and induction of resonant absorption of electromagnetic waves [3].

Advanced targets enhancing the absorption coefficient permit to transfer more energy from the laser light to the target and to the plasma and, consequently, to develop a strong ion acceleration field at the rear side of a thin target. At the laser intensity of  $10^{16}$  W/cm<sup>2</sup> the ponderomotive energy transferred to electrons from the electromagnetic wave is sufficiently high for the electrons to cross the thin target and produce TNSA effect, as it will be presented and discussed.

## 2. Experimental set-up

The experiments were carried out with the use of the PALS laser in Prague with laser pulse duration of 300 ps and fundamental wavelength of 1.3  $\mu$ m, and of a very fast and sophisticated plasma diagnostics permitting detailed analysis of the accelerated ions [4]. The plasma was generated by the laser beam focused to a focal spot 70  $\mu$ m in diameter on different planar solid targets mounted on a suitable holder. Thin targets with thickness from 0.1  $\mu$ m up to 50  $\mu$ m were employed, such as metals of different atomic numbers, polymers and ceramics, and advanced targets containing nanostructures. Generally, the laser beam was directed perpendicularly to the target surface with a laser pulse energy  $E_L \approx 100$  J  $\div$  600 J using different focal positions (FP) with respect to the target surface, from +500  $\mu$ m (focus inside the target) up to -500  $\mu$ m (focus in front of the target). Vacuum in the experimental chamber was at a level of  $5 \times 10^{-6}$  Torr.

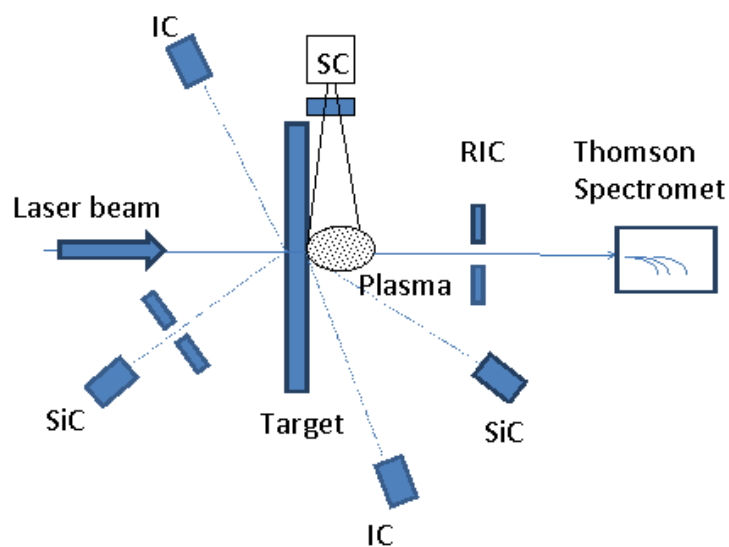


**Figure 1.** Schematic of the experimental set-up.

Ion collectors (IC) and ring ion collectors (RIC) with four different sectors using thin Al absorber films were employed to reduce the background coming from photons, electrons and ions and to separate protons from heavier ions. SiC detectors with 100  $\mu$ m depletion layer Schottky barrier were employed in time-of-flight (TOF) configuration to detect energetic ions [5]. A Ni<sub>2</sub>Si surface metallization is employed; it absorbs protons with an energy lower than 50 keV and Al ions with an energy lower than 350 keV. The SiC depletion layer depth permits to detect very well protons up to a maximum energy of about 10 MeV and Al ions with energy above 100 MeV. An X-ray streak camera (SC), with 2 ns exposition time and 30 ps time resolution, mounted in a side view, was employed for the FP distance evaluation. Details on the streak camera used are given in literature [6]. A Thomson parabola spectrometer (TPS) was employed as a fast measuring tool for analysis of the magnetically and electrically deflected ions in dependence on their mass-to-charge ratio. The spectrometer exploited a multi-channel plate coupled to a phosphorous screen and a CCD camera. The detected

parabolas were identified by using a simulation program based on Opera 3D-Tosca taking in account the real dimension of the spectrometer and real values of the magnetic and electric field considering also their edge effects. Details on the IC, SiC, streak camera and Thomson parabola spectrometer employed in this experiment are given in previous papers [5-7].

The detectors were placed at different angles with respect to the target surface, both in backward and in forward directions, in order to study the ion emission in different irradiation conditions. A typical scheme of the experimental set-up, for irradiation at  $0^\circ$  incidence angle and TNSA approach, is shown in Fig. 1.

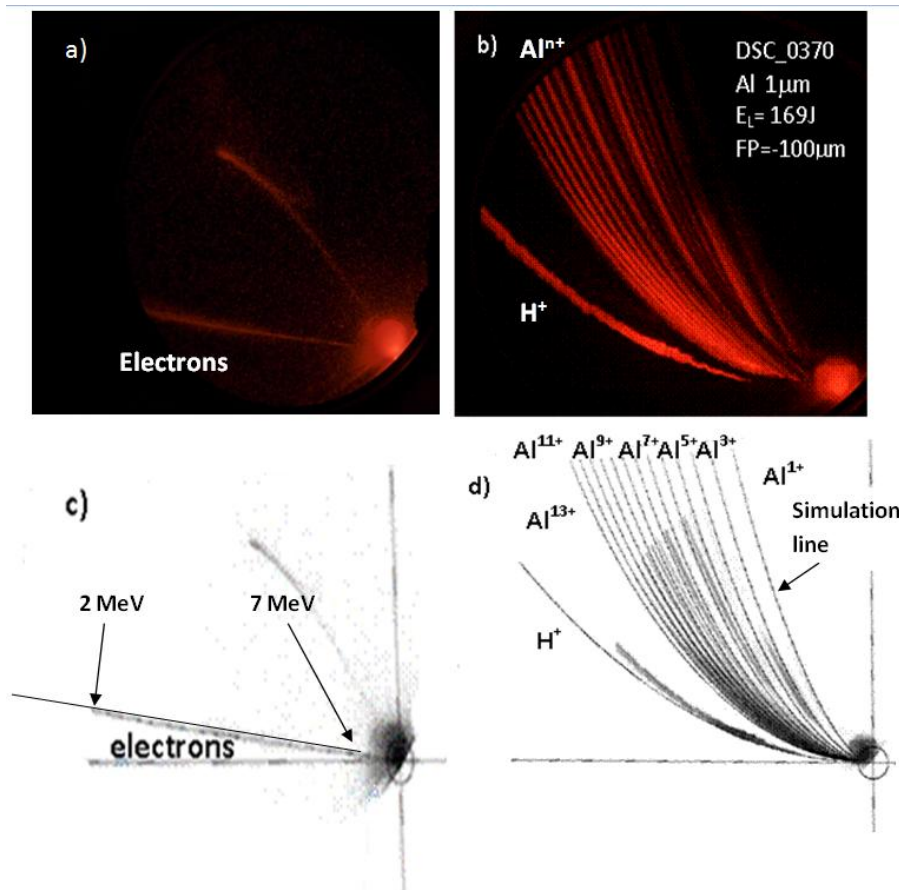


**Figure 2.** TPS spectra of fast electrons (a) and Al ions (b) and corresponding simulations (c, d).

### 3. Results

In order to confirm that the electrons emitted from a thin target in forward direction are responsible for the double layer creation and ion acceleration, TPS and SiC detectors were placed at  $0^\circ$  to monitor the electrons generated during the laser-matter interaction.

Fig. 2 shows two typical sets of parabolas obtained for  $1 \mu\text{m}$  Al target irradiation in TNSA conditions at 170 J laser pulse energy and  $-100 \mu\text{m}$  FP distance, for electrons (a) and ions (b), and the corresponding simulated parabolas (line simulations overlapped to the experimental data) for electrons (c) and ions (d), respectively. The electrons were analysed by using electric deflectors charged to 2,8 kV, and a very weak magnetic field of only 50 G. The comparison of the experimental parabola (a) and the simulation one (c) shows that the electrons from 7 MeV up to 2 MeV are detected. Such high-energy electrons accelerated in the forward direction along the normal to the target surface are responsible for the electric field developed in a double layer at the rear side of a thin TNSA target.

The TPS ion diagnostics was performed using a 1.4 kV/cm electric and 0.06 T magnetic fields. The TPS spectrum for ions (b) for the case of the 1  $\mu\text{m}$  Al film target shows protons and all the 13 charge states of aluminum. The recognition of the ion species, charge state and energy was based on the simulation data. In this case the maximum proton energy was about 3.3 MeV and the Al ion energy of about 3 MeV/charge state, in agreement with the values obtained from direct ion detection by SiC detectors.

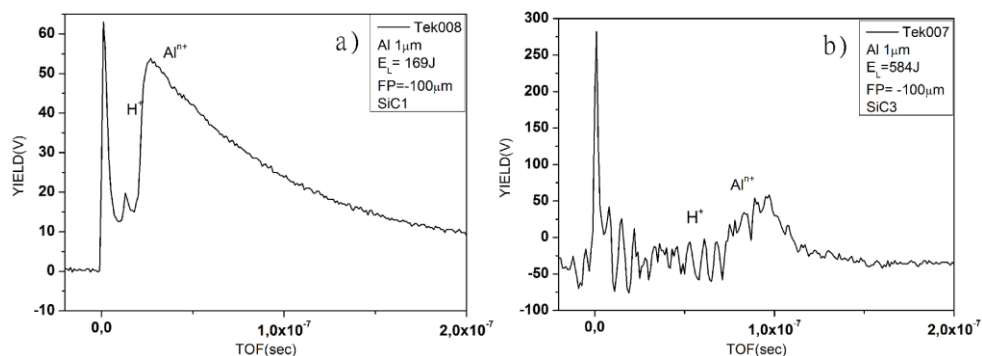


**Figure 3.** Typical SiC TOF signals for ion detection in forward (a) and in backward (b) directions.

Fig. 3 shows two typical examples of SiC signals for radiation detection in the forward (a) and backward (b) directions. The signals are acquired during the laser irradiation at 170 J pulse energy and -100  $\mu\text{m}$  FP of 1  $\mu\text{m}$  Al TNSA target. They show a photopeak, a ns-scale electron signals and slower ion peaks of which the faster ones are due to the protons. The measured spectra demonstrate that a high electron yield emission occurs both in the forward and backward directions. The kinetic energies of the detected electrons are in the range 1 keV-100 keV. The maximum proton energies in the forward and backward directions are 3.5 MeV and about 1.8 MeV, respectively.

The use of advanced targets with a structure that permits to decrease the surface reflectivity, to increase the absorption radiation and to induce resonant absorption effects, and the use of special target geometries may enhance the laser energy transferred to the plasma and increase the electric field of ion drive acceleration developed on the rear side of the TNSA target.

The surface roughness, porous structures, metal/polymer multilayer and polymer containing nanostructures were investigated at various laser energies, focal positions and target thicknesses in order to reach the maximum ion acceleration in forward direction.

Measurements have indicated that an increase in the proton energy of the order of 20-30% can be obtained by changing the reflectivity and absorption coefficient of thin films [3]. An increase of the order of 30% in energy and yield has been obtained also by using metallic nanometric structures (carbon nanotubes, Cu, Ag and Au nanoparticles) embedded in thin polymeric films (PE, acrylic resins). These nanostructures induce surface plasmon resonance absorption of the incident radiation, enhancing thus the final plasma temperature and density [8]. For the laser intensity of  $10^{16}$  W/cm<sup>2</sup> the flat target thickness is crucial for obtaining the maximum proton energy and it must be optimised to reach the maximum ion acceleration, according to literature [9, 10].

Fig. 4 shows a comparison of the SiC TOF signal (a) and the corresponding spectrum of TPS parabolas (b) indicating that protons are accelerated in forward direction up to 4.5-MeV for an advanced 10- $\mu\text{m}$  Al target irradiated at a pulse energy of 600 J. This high ion acceleration has been achieved by using special target irradiation conditions.

The Al target surface was treated with sandblasting using micrometric powder grain size accelerated at 100 m/s launched against the Al surface in order to generate high roughness, responsible of the reflectivity decreasing of the irradiation laser light. The target thickness was chosen as optimal

for flat targets in order to maximize the proton acceleration in TNSA conditions using the experimental conditions above described.

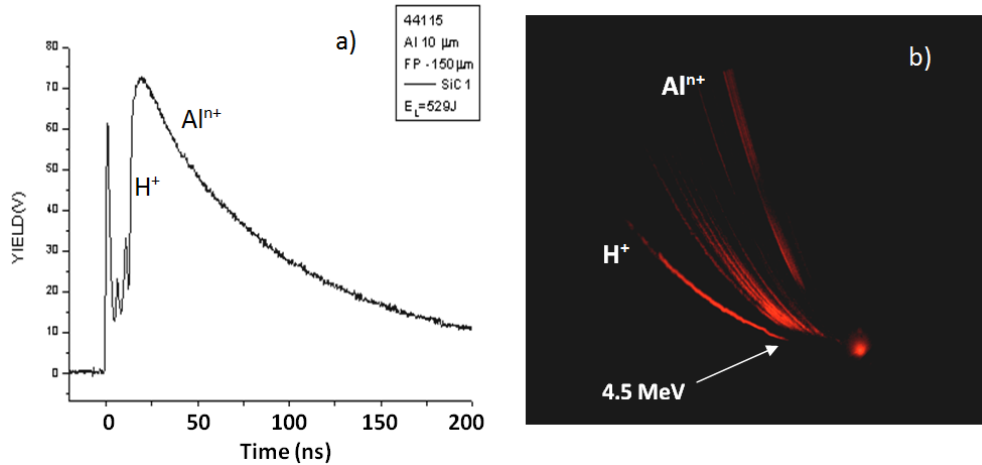


**Figure 4.** SiC signal (a) and TPS parabola spectrum (b) indicating a maximum proton energy of 4.5 MeV.

As seen in Fig. 5a, at 10 μm target thickness the proton energy reaches the maximum value. If the target is too thin or thick the electron density of plasma decreases. Moreover the protons loose energy in thick plasmas and their final energy decreases. The results illustrated by Fig. 4 were obtained for the focal position of – 150 μm in front of the target surface, at which the conditions for beam self-focusing are fulfilled. The self-focusing is due to the pre-plasma formation with high refraction index in front of the target surface, which results in reduction of the laser spot dimension on the target surface to values of the order of a single wavelength and in substantial enhancement of the irradiation laser intensity [2].

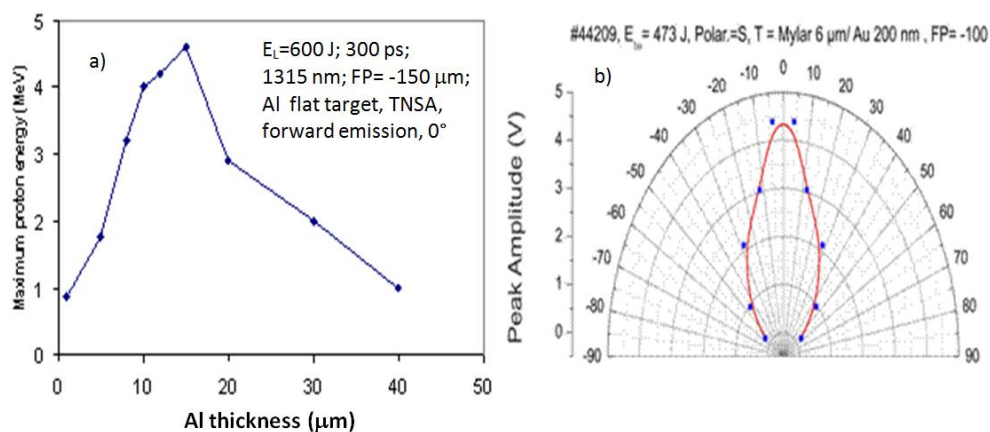


**Figure 5.** Maximum proton energy vs. Al thickness for flat targets irradiated at a 600 J and FP = -150 μm (a) and angular distribution of ions emitted in forward direction (b).

The angular distribution measurements of emitted ions performed with IC, SiC and X-ray streak camera demonstrated that under the condition of optimal thickness the forward emission occurs mainly along the normal to the target surface and that the ion stream in the forward direction is narrower than in the backward one. Fig. 5b shows a typical ion angular distribution of the ions emitted

in forward direction when laser irradiates a mylar foil in TNSA conditions, 6  $\mu\text{m}$  in thickness, covered by 200 nm of Au, by using 473 J pulse energy with -100  $\mu\text{m}$  laser beam focal position. The proton and Au ion emission occurs along the normal to the target surface with a maximum angular aperture of about  $\pm 30^\circ$ .

#### 4. Discussions and conclusions

The measurements reported in this article, performed by using the PALS facility, demonstrated that TNSA approach using 600 J laser pulse energy permits to accelerate ions in forward direction to high kinetic energies. Fast electrons of the order of 10 MeV were detected and their yield increased when using targets made of heavy metallic elements. These electrons are responsible for the high electric field driving ion acceleration. Less energetic electrons are also ejected from the target, together with the ion emission, as witnessed by SiC detectors.

About 4.5 MeV of energy per ion charge state can be obtained when irradiating thin Al targets prepared in such a way that reflectivity and absorption effects are enhanced. Thus, although the same laser and irradiation conditions were employed, significant improvement of the ion acceleration has been achieved in the last years by optimising the target composition, structure and geometry. With thick targets, for example, it was not possible to achieve more than 1 MeV per charge state still several years ago [11].

Target structure optimization plays an important role because it permits to enhance the laser energy transfer to the plasma and to increase the ion acceleration driving electric field developed in the double layers at the rear side of a thin target. Further improvements could be achieved by using polarized laser beams that permit to enhance absorption effects. When using Au nanospheres embedded in polymer, for example, the maximum proton energy was increased up to 5.0 MeV, as reported in forthcoming publication [12]. Also the advanced plasma diagnostics plays an important role at ion acceleration studies. SiC detectors and Thomson parabola spectrometry proved to be very useful in the measurements of the kinetic ion energy, charge state, angular distribution and at evaluation of the maximum electric field driving the ion acceleration.

Of course, in order to increase significantly the ion acceleration it is necessary to increase the laser intensity  $I$ , and the laser wavelength  $\lambda$ , because the acceleration field is proportional to the parameter  $I\lambda^2$  [13]. Nowadays ion acceleration of the order of 50 MeV/charge state can be obtained in the large laser facilities using PW fs lasers, at intensities exceeding  $10^{20}$  W/cm<sup>2</sup>. However also in these cases the target optimization as for its geometry, composition and structure plays an important role at attempting to increase further the ion energy, yield and directivity.

#### Acknowledgements

The authors wish to thank the staff of the PALS Laboratory in Prague and all other participants of the experiment headed by Prof. L. Torrisoni, and gratefully acknowledge the financial support given to the project by LASERLAB-EUROPE (GA 284464, EC's Seventh Framework Programme) and by the Czech Ministry of Education, Youth and Sports (project PALS RI, LM2010014).

#### References

- [1] D. Giulietti and L.A. Gizzi, *La Rivista del Nuovo Cimento* 21, 1-103, 1998
- [2] L. Torrisoni, D. Margarone, L. Laska, J. Krasa, A. Velyhan, M. Pfeifer, J. Ullschmied, L. Ryc *Laser and Particle Beams* 26, 379-387, 2008
- [3] L. Torrisoni, M. Cutroneo, F. Caridi and C. Gentile *Laser and Particle Beams* 31(01), 37 – 44, 2013
- [4] PALS web site, Prague 2013: <http://www.pals.cas.cz/laser/>
- [5] M. Cutroneo, P. Musumeci, M. Zimbone, L. Torrisoni, F. La Via, D. Margarone, A. Velyhan, J. Ullschmied and L. Calcagno, *J. Material Research* 28(01), 87 – 93, 2012
- [6] L. Láška, J. Badziak, K. Jungwirth, M. Kálal, J. Krása, E. Krouský, P. Kubeš, D. Margarone,

- P. Parys, M. Pfeifer, K. Rohlena, M. Rosinski, L. Ryc, J. Skála, L. Torrisci, J. Ullschmied, A. Velyhan, J. Wolowski *Rad. Eff. & Defects in Solids: Inc. Plasma Sci. & Plasma Tech.* 165(6–10), 463–471, 2010
- [7] M. Cutroneo, L. Torrisci, L. Andò, S. Cavallaro, J. Ullschmied, J. Krasa, D. Margarone, A. Velyhan, E. Krousky and M. Pfeifer, *Acta Polytechnica* 53(2):138–141, 2013
- [8] M. Cutroneo, L. Torrisci, D. Margarone, A. Picciotto, *Applied Surface Science* 272, 50–54, 2013
- [9] L. Torrisci, M. Cutroneo, L. Andò, and J. Ullschmied, *Phys. Plasmas* **20**, 023106, 2013
- [10] J. Fuchs, P. Antici, E. d’Humie`res, E. Lefebvre, M. Borghesi, E. Brambrink, C.A. Cecchetti, M. Kaluza, V. Malka, M. Manclossi, S. Meyroneinc, P. Mora, J. Schreiber, T. Toncian, H.P. Epinand, P. Audebert, *Nat. Phys.* 2, 48–54, 2006
- [11] L. Laska, S. Cavallaro, K. Jungwirth, J. Krasa, E. Krousky, D. Margarone, A. Mezzasalma, M. Pfeifer, K. Rohlena, L. Ryc, J. Skala, L. Torrisci, J. Ullschmied, A. Velyhan, G. Verona-Rinati *Eur. Phys. J. D* **54**, 487–492, 2009
- [12] L. Torrisci et Al., submitted to *Journal of Applied Physics*, 2014.
- [13] E L. Clark, K. Krushelnick, M. Zepf, F. N. Beg, M. Tatarakis, A. Machacek, M.I.K. Santala, I. Watts, P.A. Norreys, A.E. Dangor, *Phys. Rev. Lett.* 85, 1654–1657, 2000